RADIOCARBON, Vol 41, Nr 3, 1999, p 251–270

CALCULATION OF PAST DEAD CARBON PROPORTION AND VARIABILITY BY THE COMPARISON OF AMS ^{14}C AND TIMS U/TH AGES ON TWO HOLOCENE STALAGMITES

Dominique Genty[1] • Marc Massault[1] • Mabs Gilmour[2] • Andy Baker[3] • Sophie Verheyden[4] • Eddy Kepens[4]

ABSTRACT. Twenty-two radiocarbon activity measurements were made by accelerator mass spectrometry (AMS) on 2 Holocene stalagmites from Belgium (Han-stm1b) and from southwest France (Vil-stm1b). Sixteen thermal ionization mass spectrometric (TIMS) U/Th measurements were performed parallel to AMS analyses. The past dead carbon proportion (dcp) due to limestone dissolution and old soil organic matter (SOM) degradation is calculated with U/Th ages, measured calcite ^{14}C activity and atmospheric ^{14}C activity from the dendrochronological calibration curves. Results show that the dcp is different for the 2 stalagmites: between 10,800 and 4780 yr from present dcp=17.5% (σ=2.4; n=10) for Han-stm1b and dcp=9.4% (σ=1.6 ; n=6) between 3070 and 520 yr for Vil-stm1b. Despite a broad stability of the dcp during the time ranges covered by each sample, a slight dcp increase of about 5.0% is observed in the Han-stm1b sample between 8500 and 5200 yr. This change is synchronous with a calcite $\delta^{13}C$ increase, which could be due to variation in limestone dissolution processes possibly linked with a vegetation change. The dcp and $\delta^{13}C$ of the 2 studied samples are compared with 5 other modern stalagmites from Europe. Results show that several factors intervene, among them: the vegetation type, and the soil saturation leading to variable dissolution process systems (open/closed). The good correlation (R^2=0.98) between the U/Th ages and the calibrated ^{14}C ages corrected with a constant dcp validates the ^{14}C method. However, the dcp error leads to large ^{14}C age errors (i.e. 250–500 yr for the period studied), which is an obstacle for both a high-resolution chronology and the improvement of the ^{14}C calibration curves, at least for the Holocene.

INTRODUCTION

Several studies have demonstrated the great interest in speleothems (stalagmites, flowstones) for the study of paleoenvironments (Gascoyne 1992; Lauritzen 1995; Bar-Mattews et al. 1996). More recently, the study of annual-growth laminae in stalagmites has shown the great chronological and paleoclimatological potential of such deposits: annual growth laminae can be visible (Genty and Quinif 1996) or luminescent under UV light (Shopov and Dermendjiev 1990; Baker et al. 1993). However, 2 major problems still motivate research work: 1) finding a good paleoclimatic signal that can be transformed into a transfer function; and 2) checking the chronology by independent methods, especially for recent deposits where laminae can be counted. Paleoclimatic signals have already been detected, such as laminae thicknesses as indicators of paleoprecipitation (Railsback et al. 1994; Genty and Quinif 1996; Liu et al. 1997; Tan et al. 1997). Luminescence emission is also linked to rainfall (Baker et al. 1997), but such high-resolution studies require an extremely accurate chronology to calibrate the laminae signal with the instrumental climate records or historical data. For that, we can use:

1. Annual laminae counting. Generally, this cannot go very far back in time because of hiatuses or discontinuities in laminae series. The longest known laminae series is from China, where more than 1100 luminescent laminae have been counted continuously, but that is exceptional and linked with very regular climate variations such as monsoons (Tan et al. 1997).
2. Detection of the increase in ^{14}C activity due to bomb activity. However, this only gives the position of the pre-bomb period (around 1950–1955; Genty et al. 1998);
3. Excess ^{210}Pb for the last 100 yr. This method has been applied successfully to only one stalactite and needs more testing (Baskaran and Iliffe 1993).

[1]Université de Paris-Sud, Laboratoire d'Hydrologie et de Géochimie Isotopique, EP 1748, CNRS, bât. 504, F-91405 Orsay Cedex, France
[2]The Open University, Department of Earth Sciences, Milton Keynes, MK7 6AA, England
[3]University of Exeter, Department of Geography, Amory Building, Rennes Drive, EX4 4RJ Exeter, England
[4]Vrije Universiteit Brussel, WE-GISO, Pleinlaan 2, 1050 Brussel, Belgium

4. U/Th TIMS. This is problematic for young samples (i.e. a few hundred years old) because of the low ^{230}Th content, which is made worse by low uranium content samples.
5. ^{14}C AMS. This has great potential for high-resolution chronology for recent deposits, provided that the dead carbon proportion (dcp), due to the dissolution of the limestone and to the oxidation of soil organic matter (SOM), is known (its value, error and variation over time).

The limestone dissolution equation shows that half of the carbon should come from the limestone and the other half from soil CO_2. Then, the expected dead carbon proportion should be theoretically 50%. This is not what we observe. As explained in a former study (Genty and Massault 1997), dcp, up to recently, has been calculated in speleothems in different ways: 1) by measurement of the ^{14}C activity on modern stalagmites (Vogel 1983; Gewelt 1986); 2) by age-distance interpolation up to the top of the stalagmite (linear least-square fit; Broecker and Olson 1960; Gey and Hennig 1986; Railsback et al. 1994; Talma and Vogel 1992); 3) by comparison with pollen extracted from speleothems, which is an indirect way to find the age of the calcite deposit (Bastin and Gewelt 1986); and 4) by comparison with U/Th ages (Vogel 1983; Holmgren et al. 1994). From these earlier studies, the average dcp (or dilution factor q, which is its complement, and more often used by hydrologists) is 15% ± 5 (q=0.85 ± 0.05) (details in Genty and Massault 1997). More recently, using annually laminated stalagmites and the AMS technique, we have demonstrated that dcp due to limestone dissolution can be calculated with pre-bomb values obtained on ^{14}C activity time series of modern stalagmites (Genty et al. 1998, 1999). On the 3 sites already studied, the pre-bomb dcp (mid 1950s) varies from 9.0% to 12.2% ± 1.5. This shows that despite differences in climate and vegetation conditions, the pre-bomb dcp is relatively homogeneous. This study's aim is to calculate past dcp to see if it has changed during the Holocene. The study has at least 3 interests:

1. The study of hydrological and paleohydrological processes. Variation in dcp is the consequence of variation in dissolution processes in the unsaturated zone. These processes are controlled by the vegetation and climate.
2. Speleothem dating. The variation range of dcp during a specific period (i.e. Holocene) will control the error of speleothem ^{14}C ages. If dcp is stable, then AMS ^{14}C dating will be very useful for dating speleothems mainly because it is cheaper, requires less material (10 mg of calcite is sufficient), and is more convenient (laboratory preparation is much faster and simpler) than the U/Th method.
3. Construction of calibration curves. If we demonstrate that the past dcp is relatively constant and that it can be calculated with pre-bomb ^{14}C activity, as we have done on modern stalagmites, then past atmospheric ^{14}C activity could be calculated using U/Th ages and measured speleothem ^{14}C activity.

SITE AND SAMPLE DESCRIPTIONS

The 2 stalagmites chosen for investigation in this study are Vil-stm1b from the Villars cave (Dordogne, France; L = 45°30′N, l = 0°50′E, Z = 175 m), and Han-stm1b from the Han-sur-Lesse cave (Belgium; L = 50°08′N, l = 5°10′E, Z = 180 m). The Villars cave developed in Jurassic limestone, whereas the Han-sur-Lesse cave developed in Devonian limestone. Forest covers most of both sites, but the area just above Vil-stm1b is composed of grassland. Han-stm1b is 138 cm high and dark brown calcite. Vil-stm1b is composed of white calcite and is 109 cm high. Both samples are composed of an alternation of porous/compact calcite every few tens of centimeters. Growth laminae are visible on most of the upper half of Vil-stm1b.

METHODS

Mass Spectrometric Measurements

The main advantage of using AMS for ^{14}C, and TIMS for U/Th, is that very little sample is needed: 12–77 mg for AMS and 600–3000 mg for U/Th. This quantity of calcite corresponds to 2–10 yr of deposits for AMS and 5–50 yr for TIMS, depending on the sample's average vertical growth rate.

AMS ^{14}C Measurements

Calcite powders were reacted with H_3PO_4 to obtain CO_2. The gas was graphitized on iron with hydrogen at 650 °C for 100 min. Residual gas was used for stable isotope measurements on a SIRA spectrometer. Carbon atoms were counted with an accelerator mass spectrometer (Tandetron, Gif-sur-Yvette, France). Analytical errors, including laboratory errors, are ± 0.1‰ for $\delta^{13}C$ and between 0.4 and 1.0 pMC for ^{14}C activity. The blank correction is 0.4 pMC. Errors on ^{14}C ages include the dcp errors, which increase the final error by about 3 times (see below).

TIMS U/Th Measurements

TIMS U/Th measurements were done at 2 different laboratories: the Open University (England) for Vil-stm1b, and the GEOTOP Laboratory at the University of Quebec at Montreal (Canada) for Han-stm1b. Analytical procedures are summarized for both samples.

Samples were dissolved with nitric acid and spiked with a mixed ^{229}Th-^{236}U spikes (Vil-stm1b) and ^{229}Th-^{236}U-^{233}U (Han-stm1b). Uranium and thorium fractions were separated on anion exchange columns using standard techniques (Edwards et al. 1987). Both uranium and thorium were loaded onto graphite coated Re filaments and analyses carried out using Finnigan MAT262 (Vil-stm1b) and VG Sector (Han-stm1b) mass spectrometers. The former is equipped with a potential quadrupole and a secondary electron multiplier, the latter with an electrostatic analyzer and an ion-counting Daly detector. Errors were propagated from the in-run statistics and the uncertainties on the spike isotopic composition. The relatively high error on $^{230}Th/^{229}Th$ results for Vil-stm1b reflects the low count rates obtained for these small young, low uranium content samples. The detrital calculation used corrects for both uranium and thorium detrital contribution to the sample. It is assumed that the detrital component has a $^{232}Th/^{238}U$ molar ratio of 5, that the detrital uranium is in secular equilibrium, and that all the ^{232}Th is of detrital origin. Since $^{230}Th/^{232}Th$ activity ratios for all samples were >50, they can be viewed essentially as having negligible detrital input (except for U/Th-G sample at the base of Han-stm1b), hence the detrital age corrections are typically very small. Ages were calculated using the standard equation and the decay constants used for ^{234}U, ^{238}U, ^{230}Th and ^{232}Th were 2.835×10^{-6}, 1.55125×10^{-10}, 9.1952×10^{-6} and 4.9475×10^{-11} yr^{-1}, respectively.

Dead Carbon Proportion Calculations

The past dcp (dcp_{past}) of the 2 stalagmites studied was calculated as the following:

$$dcp_{past} = \left[1 - \left(\frac{a^{14}C_{int.}}{a^{14}C_{atm.\ init.}}\right)\right] \cdot 100\% \quad (1)$$

where $a^{14}C_{init.}$ is the initial ^{14}C activity of the calcite and $a^{14}C_{atm.\ init.}$ is the atmospheric ^{14}C activity of the time of deposition, they are defined by:

https://doi.org/10.1017/S003382220005712X Published online by Cambridge University Press

$$a^{14}C_{int.} = \frac{a^{14}C_{mes.}}{\exp(\lambda \cdot t)}, \quad (2)$$

with t=U/Th age in years and λ is the decay constant of ^{14}C, using 5730-yr half life where $a^{14}C_{mes.}$ is the measured calcite activity and $a^{14}C_{atm.\ init.}$ is found with the U/Th age on the calibration curves (bidecadal $\Delta^{14}C$ values of the Calib 3.0 data set; Stuiver and Kra 1986; Bronk Ramsey 1994).

Another method has been used to estimate the dcp on modern stalagmites (dcp_{modern}) (Genty et al. 1998, 1999). We briefly describe this method here as we compare and discuss modern dcp and past dcp. The calcite ^{14}C activity time series was reconstructed using modern stalagmites that possess annual growth laminae. Laminae counting permits to obtain a high resolution chronology. The ^{14}C activity curves obtained have shown that the ^{14}C peak due to nuclear weapon tests is time delayed in the stalagmites by up to 20 yr and that the decrease in the ^{14}C activity is highly variable from one site to another. The dcp_{modern} is given by the following:

$$dcp_{modern} = \left[1 - \left(\frac{a^{14}C_{mes.}}{a^{14}C_{atm.}}\right)\right] \cdot 100\% \quad (3)$$

where $a^{14}C_{mes.}$ is the pre-bomb calcite ^{14}C activity and $a^{14}C_{atm.}$ is the pre-bomb atmospheric ^{14}C activity.

Dead Carbon Proportion Errors

For equation (3) it can be reasonably assumed that the average error on dcp is 1.5% because average error on AMS measurements is 0.7%, and we suppose the same for the atmospheric measurement (Genty and Massault 1997). For equation (1), the error has been calculated using: 1) error on $a^{14}C_{mes.}$; 2) error on U/Th age; and 3) error on past atmospheric ^{14}C activity read on the dendrochronological calibration curve (Bidecadal $\Delta^{14}C$ values of the Calib 3.0 data set; Stuiver and Kra 1986; Bronk Ramsey 1994). Results show that dcp error is relatively high: 2.7% for Han-stm1b and 4.0% for Vil-stm1b (Tables 1 and 2).

RESULTS AND DISCUSSION

Dead Carbon Proportion and Calcite $\delta^{13}C$ Variations

The past dcp calculated on Vil-stm1b and Han-stm1b stalagmites gives these results (Tables 1–6):

1. Average dcp is higher for Han-stm1b (17.5%; 1σ=2.4; n=10) than for Vil-stm1b (9.4%; 1σ=1.6; n=6) (Figure 1).
2. In the Han-stm1b stalagmite, the dcp goes through a broad maximum between 8500 and 5200 yr (19.6%; 1σ=0.8; n=5) while it is about 5% lower elsewhere.
3. Vil-stm1b average dcp are within error margins.

https://doi.org/10.1017/S003382220005712X Published online by Cambridge University Press

Table 1 ^{14}C and dead carbon proportion results on Vil-stm1b stalagmite[a]

Sample name	Lab nr (PA-)	Position (cm/base)	Error (cm)	Weight (mg)	$a^{14}Cm$ (pMC)	Error (pMC)	Conv. ^{14}C age (yr BP)	Error (yr)	dcp1 (%)	Error	dcp1 corrected $a^{14}C$ (pMC)	Error (pMC)	Conv. dcp corrected ^{14}C age (yr BP)
14C-C	234	108.7	0.2	22.5	96.6	1.0	270	80	9.4	1.5	106.7	2.5	
14C-H	276	106.2	0.2	12.2	86.5	0.9	1160	80	9.4	1.5	95.5	2.4	368
14C-L	290	101.3	0.2	43.1	86.4	0.7	1170	60	9.4	1.5	95.4	2.2	380
14C-G	275	91	0.2	28.7	87.4	0.7	1080	60	9.4	1.5	96.5	2.2	
14C-K	289	80.4	0.2	34.9	83.6	0.6	1440	60	9.4	1.5	92.3	2.1	650
14C-B	233	71	0.2	35.6	76.3	1.0	2170	110	9.4	1.5	84.2	2.5	1380
14C-J	288	59.5	0.2	23.9	74.9	0.6	2320	60	9.4	1.5	82.7	2.1	1530
14C-I	287	42.5	0.2	15.9	68.6	0.6	3030	70	9.4	1.5	75.7	2.1	2240
14C-F	274	24.6	0.2	25	65.1	0.6	3450	60	9.4	1.5	71.8	2.1	2660
14C-E	273	5	0.2	27	63.4	0.6	3660	70	9.4	1.5	70.0	2.1	2860
14C-A	232	1.5	0.2	77.6	62.3	0.6	3800	70	9.4	1.5	68.7	2.1	3010

Sample name	Error (yr)	Calib. cor. ^{14}C age yr AD/(−)BC	Error + yr AD/(−)BC	Error − yr AD/(−)BC	U/Th ages yr AD/(−)BC	$\Delta^{14}C_{atm.}$ (‰)	Error (‰)	$a^{14}C_{atm.}$ (pMC)	Error (pMC)	$a^{14}C_{init.}$ (pMC)	Error (pMC)	dcp (%)	Error (%)
14C-C		1990	1989	1991									
14C-H	200	1940	1937	1943									
14C-L	180	1935	1800	1993									
14C-G					1480	8.8	2	100.88	0.2	93.1	3.2	7.7	3.4
14C-K	180	1310	1160	1460	1320	−12.8	1.6	98.72	0.16	90.8	4.9	8.1	5.1
14C-B	240	675	400	950	620	−18.7	2.1	98.13	0.21	90.1	4.4	8.2	4.6
14C-J	200	510	320	700	760	−16.4	1.3	98.36	0.13	87.0	3.0	11.5	3.1
14C-I	220	−250	−550	50									
14C-F	230	−725	−1050	−400	−590	−2.7	1.7	99.73	0.17	89.0	3.7	10.8	3.9
14C-E	240	−1100	−1400	−800									
14C-A	240	−1225	−1550	−900	−1070	3.8	1.8	100.38	0.18	90.3	3.5	10.1	3.7

[a] a^{14}_m = measured ^{14}C activity; dcp1 = averaged past dead carbon proportion (see text); Calibration of ^{14}C ages have been done with OxCal v2.8 program (Stuiver and Kra 1986; Bronk Ramsey 1994); $\Delta^{14}C_{atm.}$ and $a^{14}_{atm.}$ = atmospheric ^{14}C activity of the known age deposit (grace to U/Th age) from calibration curves; dcp = calculated dead carbon proportion using U/Th ages, a^{14}_m and $a^{14}_{atm.}$ (past dcp).

Table 2 ^{14}C and dead carbon proportion results on Han-stmlb stalagmite[a]

Sample name (^{14}C-)	Lab nr (PA-)	Position (cm/base)	Error (cm)	Weight (mg)	$a^{14}Cm$ (pMC)	Error (pMC)	Conv. ^{14}C age (yr BP)	Error (yr)	dcp1 (%)	Error	dcp1 corrected $a^{14}C$ (pMC)	Error (pMC)	Conv. dcp corrected ^{14}C age (yr BP)
G	376	3	0.1	25.1	19.8	0.4	13,020	160	17.5	1.5	24.0	1.9	11,480
A	291	12.3	0.1	14.3	25.5	0.5	10,990	160	17.5	1.5	30.9	2.0	9440
E	302	33	0.1	15.5	27.7	0.4	10,300	110	17.5	1.5	33.6	1.9	8760
B2	293	43.5	0.1	11.4	28.2	0.7	10,180	200	17.5	1.5	34.1	2.2	8630
B1	292	54.3	0.1	23.2	30.6	0.5	9510	130	17.5	1.5	37.1	2.0	7970
H	378	67	0.1	26.5	30.9	0.5	9430	110	17.5	1.5	37.5	2.0	7880
C	294	93.7	0.1	24.5	36.5	0.4	8090	90	17.5	1.5	44.3	1.9	6540
I	379	101	0.1	23.6	37.2	0.5	7940	100	17.5	1.5	45.1	2.0	6390
F	303	108.9	0.1	11.6	39.8	0.4	7410	90	17.5	1.5	48.2	1.9	5870
D	301	129.4	0.1	21.3	45.5	0.4	6330	70	17.5	1.5	55.1	1.9	4790
J	380	137.7	0.1	29.6	50.7	0.4	5460	60	17.5	1.5	61.4	1.9	3910

Sample name (^{14}C-)	Error (yr)	Calibrated cor. ^{14}C age (BC)	Error (+ BC)	Error (− BC)	U/Th ages (BC)	$\Delta^{14}C_{atm.}$ (‰)	Error (‰)	$a^{14}C_{atm.}$ (pMC)	Error (pMC)	$a^{14}C_{init.}$ (pMC)	Error (pMC)	dcp (%)	Error (%)
G	640	11,550	12,300	10,800									
A	520	8750	9600	7900	8690	127.4	2.9	112.74	0.29	92.7	2.7	17.8	3.0
E	450	7750	8400	7100	8060	109.7	2.2	110.97	0.22	93.7	2.2	15.6	2.5
B2	520	7700	8400	7000	8010	101.9	1.9	110.19	0.19	94.5	3.2	14.2	3.4
B1	430	6925	7450	6400	7080	89.9	4.9	108.99	0.49	91.7	2.6	15.8	3.1
H	420	6750	7300	6200	6520	63.6	1.8	106.36	0.18	86.6	2.0	18.6	2.2
C	340	5400	5750	5050	5140	89.9	1.7	108.99	0.17	86.6	2.0	20.5	2.2
I	360	5275	5650	4900	5210	97.6	2.7	109.76	0.27	89.0	2.5	18.9	2.8
F	320	4775	5200	4350	4390	75.4	2.3	107.54	0.23	86.1	3.2	19.9	3.4
D	280	3525	3950	3100	3220	67.5	1	106.75	0.1	85.5	2.1	20.0	2.2
J	250	2350	2700	2000	2780	53.1	1.4	105.31	0.14	90.3	1.4	14.2	1.5

[a] a^{14}_m = measured ^{14}C activity; dcp1 = averaged past dead carbon proportion (see text); Calibration of ^{14}C ages have been done with OxCal v2.8 program (Stuiver and Kra 1986; Bronk Ramsey 1994); $\Delta^{14}C_{atm.}$ and $a^{14}_{atm.}$ = atmospheric ^{14}C activity of the known-age deposit (grace to U/Th age) from calibration curves; dcp = calculated dead carbon proportion using U/Th ages, a^{14}_m and $a^{14}_{atm.}$ (past dcp).

Table 3 U/Th results of Vil-stm1b stalagmite[a]

Sample name	Position (cm/base)	Error (cm)	^{238}U (ppm)	Error (ppm)	$^{234}U/^{238}U$ act.	Error act.	^{234}U (ppm)	Error (ppm)	^{230}Th (ppb)	Error (ppb)
U/Th-G	96	0.3	0.13040	0.00054	0.99385	0.00718	6.97E-06	5.05E-08	7.88E-06	3.58E-07
U/Th-C	91	0.3	0.13802	0.00013	1.0025	0.01888	7.44E-06	1.86E-08	1.10E-05	1.74E-07
U/Th-H	79.7	0.3	0.13547	0.0003	0.99671	0.00481	7.26E-06	3.55E-08	1.40E-05	5.69E-07
U/Th-F	70.7	0.3	0.15365	0.00064	0.94893	0.01278	7.84E-06	1.09E-07	3.03E-05	7.32E-07
U/Th-B	59.5	0.3	0.09428	0.00007	1.0052	0.0189	5.10E-06	1.25E-08	1.76E-05	2.85E-07
U/Th-E2	24.6	0.3	0.14071	0.00021	1.00498	0.01930	7.61E-06	2.49E-08	5.43E-05	1.33E-06
U/Th-A	1.5	0.3	0.12185	0.00043	1.0762	0.0276	7.05E-06	1.24E-07	5.99E-05	5.88E-07

Sample name	^{232}Th (ppb)	Error (ppb)	$^{230}Th/^{232}Th$ act.	Error act.	$^{230}Th/^{234}U$ act.	Error act.	Row age (yr/present)	Error (yr)	Cor. age (yr/present)	Error	% error (1σ)
U/Th-G	0.02706	0.00016	71.53	3.28	0.00373	0.00017	410	20	400	20	5.2
U/Th-C	0.0812	0.0001	50.58	0.80	0.00488	0.00013	530	15	520	15	2.6
U/Th-H	0.06748	0.0003	64.96	2.66	0.00636	0.00026	690	30	680	30	4.6
U/Th-F	0.15442	0.00025	62.89	1.52	0.01277	0.00036	1400	40	1370	40	3.6
U/Th-B	0.0197	0.0001	236.41	4.01	0.01137	0.0003	1240	35	1240	35	2.7
U/Th-E2	0.0383	0.00034	306.13	7.99	0.02354	0.00077	2590	85	2590	85	3.3
U/Th-A	0.1457	0.0002	89.71	0.89	0.02804	0.00082	3090	90	3070	90	3

[a]Act. = activity; Cor. Age = detrital corrected U/Th age. Error margins are 1σ.

Table 4 U/Th results of Han-stmlb stalagmite[a]

Sample name (U/Th-)	Position cm/base	Error (cm)	^{238}U (ppm)	Error (ppm)	^{232}Th (ppb)	Error (ppb)	$^{234}U/^{238}U$ act.	Error act.	$^{230}Th/^{234}U$ act.	Error act.	Cor. age (yr/present)	Error
G	1.75	0.90	1.34340	0.00477	281.460	6.60110	1.87040	0.0095	—	—	—	—
A	12.10	0.90	1.5877	0.00588	7.6749	0.0287	1.8487	0.01	0.0942	0.0009	10,680	110
E	32.90	0.60	1.7961	0.0082158	1.7748	0.0077535	1.8227	0.0112	0.0889	0.0008	10,060	95
B2	43.50	0.60	1.7778	0.0057904	1.7456	0.0069017	1.8212	0.0105	0.0885	0.0008	10,010	95
B1	54.30	0.70	1.3398	0.00594	15.235	0.05296	1.7538	0.0102	0.0805	0.0009	9070	105
H	66.95	0.95	1.2331	0.0046701	3.0343	0.01142	1.7247	0.0088	0.0757	0.0006	8520	70
C	93.80	0.4	0.83868	0.0035	14.84	0.059	1.7396	0.0121	0.0638	0.0008	7140	90
I	101.00	1.00	0.90814	0.0033586	12.828	0.07443	1.7982	0.0132	0.0644	0.0009	7210	105
F	108.80	0.6	0.93735	0.0049	10.7	0.071	1.7574	0.0161	0.0573	0.0015	6392	172
D	129.45	0.55	0.90229	0.00312	4.3076	0.013419	1.7457	0.0094	0.047	0.0007	5220	80
J	136.10	1.60	1.0657	0.00397	1.4631	0.0051206	1.7113	0.0102	0.0431	0.0003	4780	35

[a]Act. = activity; Cor. Age = detrital corrected U/Th age. Error margins are 1 σ.

Dcp Difference between Han-stm1b and Vil-stm1b Stalagmites

Differences between averaged dcp in Han-stm1b and Vil-stm1b can be due to numerous causes:

1. Differences in limestone dissolution processes (i.e. difference in the relative importance of open/closed systems; Hendy 1971; Dulinski and Rozanski 1990) due to differences in the soil and host rock characteristics (porosity, thickness) and/or in climate and vegetation conditions.
2. A different time residence of the seepage water. The longer the water stays in the micro-fissure network, the more limestone is dissolved and the dead-carbon proportion is greater. The residence time of the water can be controlled by the limestone thickness above the studied site. Because limestone thickness above Han-stm1b is 50 m while it is 10 m above Vil-stm1b, it is possible that this thickness variation explains the higher dcp for the Han-stm1b sample.

Table 5 $\delta^{13}C$ of Vil-stmlb stalagmite

Sample name	Position (cm/base)	U/Th age	Estimated error (–yr)	$\delta^{13}C$ (‰ PDB, ±0.1)
Vil-stm1-0	0.00	–1100 BC	90	–10.80
Vil-stm1-2	2.00	–1060 BC	90	–10.77
Vil-stm1-4	4.00	–1020 BC	90	–10.45
Vil-stm1-10	10.00	–900 BC	90	–10.65
Vil-stm1-20	20.00	–680 BC	85	–10.42
Vil-stm1-30	30.00	–380 BC	80	–11.09
Vil-stm1-40	40.00	10 AD	70	–10.77
Vil-stm1-50	50.00	400 AD	50	–11.32
Vil-stm1-60	60.00	750 AD	30	–9.88
Vil-stm1-74	74.00	860 AD	50	–8.39
Vil-stm1-80	80.00	1315 AD	30	–8.72
Vil-stm1-90	90.00	1470 AD	15	–10.01
Vil-stm1-100	100.00	1870 AD	15	–9.74
Vil-stm1-106	106.00	1940 AD	10	–8.84

Except for the high dcp (30–35%) found in a stalagmite from Castelguard cave (Canada) where no soil develops (Gascoyne and Nelson 1983), the past dcp found in Han-stm1b and Vil-stm1b is in agreement with the already published dcp found in modern speleothems from temperate countries (15% ± 5; see above for references). The dead carbon proportion (or the dilution factor q, which is its correlant, often used by hydrologists [q=(100–dcp)/100)], is the consequence of limestone dissolution processes in the unsaturated zone. Limestone dissolution can occur, theoretically, under 2 processes called open and closed systems (Hendy 1971), or coincident and sequential systems (Drake 1983, 1984). In an open system, the seepage water is in contact with soil CO_2 during limestone dissolution, while in a closed system, dissolution occurs when the seepage water is isolated from soil CO_2. In the first case, dissolved inorganic carbon (DIC) (HCO_3^-), which comes from limestone dissolution, is changed by dissolved CO_2 which can be degassed; consequently, old C can be removed from the seepage water leading toward a low dcp. In the second case (closed system), limestone dissolution, which brings the dead carbon in the water, is limited by the quantity of dissolved CO_2 which is itself controlled by the soil pCO_2. After complete dissolution, theoretical dcp goes up to 50%.

Soils in karst areas are generally very thin (5–20 cm thick) and carbonate is quickly reached by the infiltrated water, so consequently the 3 phases (CO_2, water, and limestone) are gathered, and an open system is more likely to occur, at least during the first stage of seepage. During water infiltration, the

https://doi.org/10.1017/S003382220005712X Published online by Cambridge University Press

Table 6 $\delta^{13}C$ of Han-stmlb stalagmite

Position (cm/base)	Interpolated U/Th ages (yr present)	$\delta^{13}C$ ‰ PDB (± 0.1)	Position (cm/base)	Interpolated U/Th ages (yr present)	$\delta^{13}C$ ‰ PDB (± 0.1)	Position (cm/base)	Interpolated U/Th ages (yr present)	$\delta^{13}C$ ‰PDB (± 0.1)	Position (cm/base)	Interpolated U/Th ages (yr present)	$\delta^{13}C$ ‰PDB (± 0.1)
3	10,949	−6.80	37	10,039	−7.23	71	8312	−6.95	105	6798	−6.31
4	10,920	−7.20	38	10,035	−6.89	72	8261	−6.45	106	6696	−6.34
5	10,890	−7.18	39	10,030	−7.24	73	8210	−5.98	107	6594	−6.07
6	10,860	−7.49	40	10,025	−6.94	74	8159	−6.18	108	6492	−6.16
7	10,831	−7.10	41	10,020	−7.08	75	8108	−6.63	109	6390	−6.35
8	10,801	−7.44	42	10,016	−6.94	76	8057	−6.34	110	6331	−6.37
9	10,771	−7.12	43	10,011	−6.98	77	8006	−6.37	111	6273	−6.40
10	10,741	−7.39	44	9926	−7.14	78	7955	−6.70	112	6214	−6.43
11	10,712	−7.15	45	9841	−7.16	79	7904	−6.59	113	6156	−6.18
12	10,682	−7.27	46	9756	−6.80	80	7853	−6.56	114	6097	−6.44
13	10,652	−6.57	47	9671	−6.62	81	7803	−6.37	115	6039	−5.85
14	10,623	−7.09	48	9586	−6.67	82	7752	−6.31	116	5980	−5.77
15	10,593	−7.89	49	9500	−6.83	83	7701	−6.95	117	5922	−6.26
16	10,563	−7.69	50	9415	−6.92	84	7650	−6.75	118	5863	−5.88
17	10,533	−8.18	51	9330	−6.54	85	7599	−6.70	119	5805	−6.12
18	10,504	−7.67	52	9245	−6.47	86	7548	−6.73	120	5746	−6.22
19	10,474	−7.35	53	9160	−6.50	87	7497	−5.86	121	5687	−6.13
20	10,444	−7.49	54	9075	−6.34	88	7446	−5.82	122	5629	−6.11
21	10,415	−7.42	55	9032	−6.77	89	7395	−6.42	123	5570	−6.51
22	10,385	−6.86	56	8989	−6.15	90	7344	−6.45	124	5512	−6.73
23	10,355	−6.99	57	8946	−6.86	91	7293	−6.42	125	5453	−6.84
24	10,325	−7.38	58	8903	−6.21	92	7242	−6.44	126	5395	−6.81
25	10,296	−7.45	59	8860	−7.05	93	7191	−6.49	127	5336	−6.78
26	10,266	−7.45	60	8817	−6.54	94	7140	−6.39	128	5278	−6.80
27	10,236	−7.56	61	8774	−6.70	95	7149	−6.39	129	5219	−6.72
28	10,207	−7.19	62	8731	−6.61	96	7159	−6.62	130	5164	−6.59
29	10,177	−7.23	63	8688	−6.50	97	7168	−6.77	131	5109	−6.62
30	10,147	−7.27	64	8645	−6.88	98	7178	−6.82	132	5054	−6.77
31	10,117	−6.85	65	8602	−7.01	99	7187	−7.06	133	4999	−6.43
32	10,088	−7.35	66	8559	−7.00	100	7197	−7.00	134	4943	−6.26
33	10,058	−7.17	67	8516	−6.98	101	7206	−5.91	135	4888	−6.81
34	10,053	−7.55	68	8465	−6.91	102	7104	−6.12	136	4833	−6.60
35	10,049	−7.82	69	8414	−6.83	103	7002	−6.09	137	4778	−6.46
36	10,044	−7.79	70	8363	−6.67	104	6900	−6.16			

CO_2 gas volume in contact with water and limestone decreases and dissolution conditions become closer to the closed system conditions. As explained by earlier studies (Hendy 1971; Drake 1984), the real situation in the karst unsaturated zone is an intermediate between these 2 dissolution processes for 3 reasons: 1) vegetation roots penetrate the rock formation up to several meters and by their respiration they produce CO_2, which can play an important role in the pCO_2 balance and then in the dissolution process; 2) it has been demonstrated that in most karst areas the micro-fissures are filled by both water and gas, the main components of a 2-phase seepage (Mangin 1975; Fleyfel 1979; Fleyfel and Bakalowicz 1979), and this might increase the possibility of open system conditions at different depths in the karst; and 3) depending on the meteorological conditions (i.e. rainfall intensity, evapotranspiration), the seepage will be variable and exchanges between the different phases will also vary. The dead carbon difference observed between the 2 samples studied could be the consequence of a different proportion of open and closed regimes during the dissolution process.

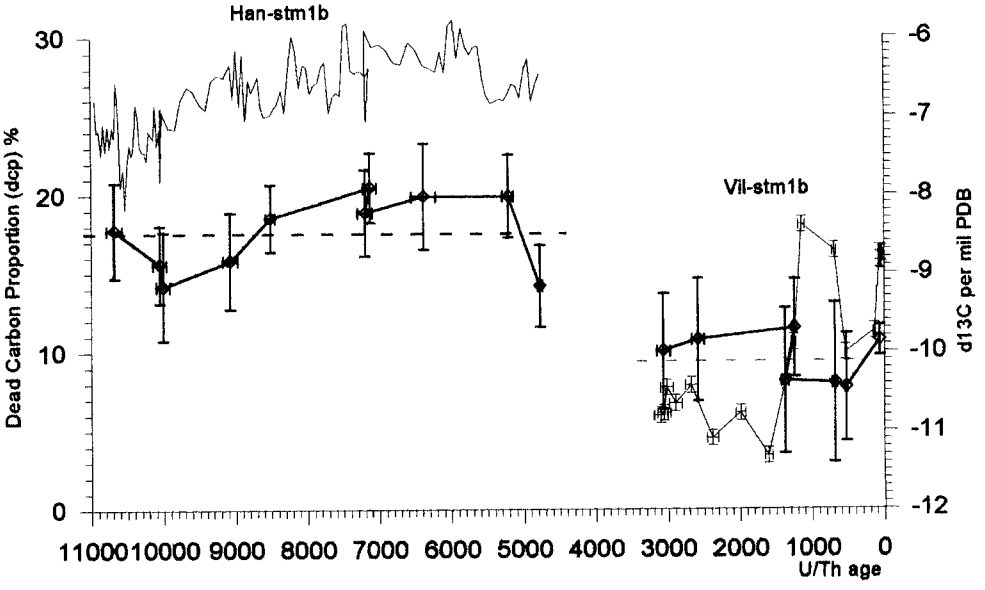

Figure 1 Dead carbon proportion (dcp) and $\delta^{13}C$ (thin lines) vs. U/Th ages of the 2 studied stalagmites. Note that for each stalagmite, the dcp stays relatively stable during the growth: average dcp is 17.5% (σ=2.4%; n=10) for Han-stm1b and is 9.4% (σ=1.6% ; n=6) for Vil-stm1b. However, we note a slight increase of the dcp and of the $\delta^{13}C$ between 8500 and 5200 yr for Han-stm1b. This could be the consequence of a vegetation change (see text).

$\delta^{13}C$ Differences between Han-stm1b and Vil-stm1b Stalagmites

Because limestone $\delta^{13}C$ is much higher than soil $\delta^{13}C$ (between –2‰ and +2‰, and between –20‰ and –24‰ for soil CO_2 under C3 plants), $\delta^{13}C$ measurements in the precipitated calcite give useful information about the sources of the DIC species, and consequently on the dissolution processes. The ^{13}C content of the precipitated calcite in speleothems is controlled by the following:

1. Soil CO_2 $\delta^{13}C$, which depends on the photosynthetic pathway and hence on the vegetation type: under C3 plants $\delta^{13}C$ is about –22‰, whereas it is about –12‰ for C4 plants (Dever et al. 1982; Dörr and Münnich 1986; Fleyfel 1979; Hendy 1971).
2. The temperature, which controls the isotope fractionation between soil CO_2 and DIC (Mook et al. 1974), and between DIC and precipitated $CaCO_3$ (Mook 1980).
3. The quantity of dissolved limestone and its $\delta^{13}C$ (–1.2‰ for Han-sur-Lesse site, –1.9‰ for Villars site), controlled by the dissolution process (open/closed system proportions).

https://doi.org/10.1017/S003382220005712X Published online by Cambridge University Press

Table 7 Calculation of the theoretical calcite $\delta^{13}C$ under different environmental conditions using a mixing model (dcp) and isotopic fractionation factors (see text for details)[a]

	Temp. (°C)	Soil $\delta^{13}C$	$\delta^{13}C$ <diss.	dcp (%)	Limestone $\delta^{13}C$	$\delta^{13}C$ >diss.	$CaCO_2$ $\delta^{13}C$
A							
Villars site	10	−20.30	−10.70	9.40	−1.90	−9.87	−9.72
	11	−20.30	−10.82	9.40	−1.90	−9.98	−9.77
	12	−20.30	−10.93	9.40	−1.90	−10.08	−9.83
	13	**−20.30**	**−11.05**	**9.40**	**−1.90**	**−10.19**	**−9.88**
	14	−20.30	−11.17	9.40	−1.90	−10.29	−9.93
	15	−20.30	−11.28	9.40	−1.90	−10.40	−9.99
	16	−20.30	−11.39	9.40	−1.90	−10.50	−10.04
Han-sur-Lesse site	6	−17.80	−7.72	17.50	−1.20	−6.58	−6.64
	7	−17.80	−7.84	17.50	−1.20	−6.68	−6.68
	8	−17.80	−7.96	17.50	−1.20	−6.78	−6.73
	9	**−17.80**	**−8.08**	**17.50**	**−1.20**	**−6.88**	**−6.78**
	10	−17.80	−8.20	17.50	−1.20	−6.97	−6.82
	11	−17.80	−8.32	17.50	−1.20	−7.07	−6.86
	12	−17.80	−8.43	17.50	−1.20	−7.17	−6.91
B							
Villars site	13	−17.00	−7.75	9.40	−1.90	−7.20	−6.89
	13	−18.00	−8.75	9.40	−1.90	−8.11	−7.80
	13	−19.00	−9.75	9.40	−1.90	−9.01	−8.70
	13	**−20.00**	**−10.75**	**9.40**	**−1.90**	**−9.92**	**−9.61**
	13	**−21.00**	**−11.75**	**9.40**	**−1.90**	**−10.82**	**−10.51**
	13	−22.00	−12.75	9.40	−1.90	−11.73	−11.42
	13	−23.00	−13.75	9.40	−1.90	−12.64	−12.33
Han-sur-Lesse site	9	−15.00	−5.28	17.50	−1.20	−4.57	−4.47
	9	−16.00	−6.28	17.50	−1.20	−5.39	−5.29
	9	**−17.00**	**−7.28**	**17.50**	**−1.20**	**−6.22**	**−6.12**
	9	**−18.00**	**−8.28**	**17.50**	**−1.20**	**−7.04**	**−6.94**
	9	−19.00	−9.28	17.50	−1.20	−7.87	−7.77
	9	−20.00	−10.28	17.50	−1.20	−8.69	−8.59
	9	−21.00	−11.28	17.50	−1.20	−9.52	−9.42
C							
Villars site	13	−20.30	−11.05	5.00	−1.90	−10.59	−10.28
	13	−20.30	−11.05	7.00	−1.90	−10.41	−10.10
	13	**−20.30**	**−11.05**	**9.00**	**−1.90**	**−10.23**	**−9.92**
	13	−20.30	−11.05	11.00	−1.90	−10.04	−9.73
	13	−20.30	−11.05	13.00	−1.90	−9.86	−9.55
	13	−20.30	−11.05	15.00	−1.90	−9.68	−9.37
	13	−20.30	−11.05	17.00	−1.90	−9.49	−9.18
Han-sur-Lesse site	9	−17.80	−8.08	12.00	−1.20	−7.25	−7.15
	9	−17.80	−8.08	14.00	−1.20	−7.12	−7.02
	9	−17.80	−8.08	16.00	−1.20	−6.98	−6.88
	9	**−17.80**	**−8.08**	**18.00**	**−1.20**	**−6.84**	**−6.74**
	9	−17.80	−8.08	20.00	−1.20	−6.70	−6.60
	9	−17.80	−8.08	22.00	−1.20	−6.57	−6.47
	9	−17.80	−8.08	24.00	−1.20	−6.43	−6.33
D							
Han-sur-Lesse site	6	**−18.40**	**−8.32**	14.20	**−1.20**	**−7.31**	**−7.37**
	10	**−17.40**	**−7.80**	**20.50**	**−1.20**	**−6.45**	**−6.29**

[a]**A**: T changes, soil $\delta^{13}C$ and dcp are constant. **B**: soil $\delta^{13}C$ changes, T and dcp are constant. **C**: dcp changes, T and soil $\delta^{13}C$ are constant. **D**: temperature, soil $\delta^{13}C$ and dcp changes to take into account the observed calcite $\delta^{13}C$ variation in the Han-stm1b stalagmite (see text). Numbers in bold correspond to our measurements.

https://doi.org/10.1017/S003382220005712X Published online by Cambridge University Press

As Figure 1 shows, similar to the dcp, the average $\delta^{13}C$ is higher in Han-stm1b (–6.7‰; σ=0.5; n=135) than in Vil-stm1b (–9.8‰; σ=1.1; n=17). We have calculated the theoretical precipitated calcite $\delta^{13}C$ using a simple mixing model (dcp for limestone dissolution; see Genty et al. 1999 for details) and hypotheses have been made for temperature, soil CO_2 $\delta^{13}C$ and dcp variations (Table 7). Apparently, the main factor that controls the calcite $\delta^{13}C$ is soil $\delta^{13}C$, and reasonable changes in temperature (±3 °C, which is much higher than the Holocene temperature variation) and in dcp do not significantly change the calcite $\delta^{13}C$. For Vil-stm1b, the theoretical calcite $\delta^{13}C$ agrees well with measured $\delta^{13}C$ for a mean temperature of 13 °C and a soil CO_2 $\delta^{13}C$ of –20.5‰, which is in the range of accepted values –20‰ to –22‰ for soil under C3 vegetation (Fritz et al. 1978; Dörr and Münnich 1986 etc.). However, for the Han-stm1b stalagmite, the calculated calcite $\delta^{13}C$ can fit with the measured values only if we use a very high soil CO_2 $\delta^{13}C$ (–17.8‰). Here, reasonable variations in dcp or in temperature do not change the calculated calcite $\delta^{13}C$ sufficiently. This suggests 2 explanations. The first, a different vegetation with a higher proportion of C4 vegetation (which produces a higher soil CO_2 $\delta^{13}C$) above the Han-sur-Lesse cave, can be rejected because C4 plants characterize semi-arid climate, which did not occur during this period in Belgium (Bastin 1990; Bastin and Gewelt 1986; Lamb 1995). The second explanation is that some process enriched the Han-stm1b in ^{13}C. These processes could include 1) evaporation, unlikely because of the high humidity in the cave (close to 100%) and also because other stable isotopes ($\delta^{18}O$) satisfy the Hendy equilibrium criteria (Hendy 1971); 2) increases in closed/open system ratio or decreases in soil pCO_2 as suggested by a recent semi-dynamic model (Dulinski and Rozanski 1990); or 3) degassing and $CaCO_3$ precipitation during seepage in the unsaturated zone (Baker et al. 1997).

Table 8 Examples of dcp and $\delta^{13}C$ variations in Holocene and modern stalagmites. On modern samples, the dcp has been calculated with the ^{14}C activity curve on modern and laminated stalagmites[a]

Sample	Location	dcp (%)	Error	$\delta^{13}C$ ‰ PDB	Error	Nr of analyses	Method	Stalagmite age	Ref[b]
Fau-stm14	La Faurie (Dordogne, SW France)	9	1.5	–10.3	0.1	21	Bomb-^{14}C curve	Modern	1
Han-stm5	Han-sur-Lesse (Belgium)	12.2	1.5	–9.4	0.1	14	Bomb-^{14}C curve	Modern	2
Pos-stm4	Postojna (Slovenia)	11.6	1.5	–9.6	0.1	11	Bomb-^{14}C curve	Modern	3
Vil-stm1	Villars (SW France)	9.4	1.5	–9.9	0.1	11	U/Th-^{14}C age comparison	3.07 ka to 0 ka	3
Han-stm1	Han-sur-Lesse (Belgium)	17.5	1.5	–6.8	0.1	135	U/Th-^{14}C age comparison	11 ka to 4.8 ka	3
BFM-Boss	Brown's Folly Mine (Great Britain)	17.5	1.5	–10.0	0.1	5	Bomb-^{14}C curve	Modern	4
SU	Sutherland (Scotland)	35.5	1.5	–10.7	0.1	5	Bomb-^{14}C curve	Modern	4

[a]Genty et al. (1998) and Genty and Massault (1999)

[b]1=Genty and Massault (1999); 2=Genty et al. (1998); 3=This study; 4=Baker and Genty, unpublished.

Comparison with Other Published Stalagmite dcp and $\delta^{13}C$

To better understand the causes of the dcp and $\delta^{13}C$ variations, we compared our data with 5 more data points from stalagmites already studied and where the dcp has been calculated (Table 8 and Figure 2; Genty et al. 1998; Genty and Massault 1999; Baker and Genty, unpublished). For these new examples, the dcp was calculated with the ^{14}C activity curve reconstructed over the last 50 years

and, when possible, with annual growth laminae (visible or luminescent). The dead carbon proportion is calculated at the pre-bomb level, as explained earlier, by comparing the atmosphere and the calcite activity around 1950 AD. Figure 2 shows the following:

- 5 samples are grouped in a $\delta^{13}C$ range between –10.3‰ and –9.3‰ PDB and a dcp range between 9% and 18%;
- 1 sample has a high $\delta^{13}C$ and a relatively low dcp (Han-stm1);
- 1 sample has a low $\delta^{13}C$ and a high dcp (SU-96-7).

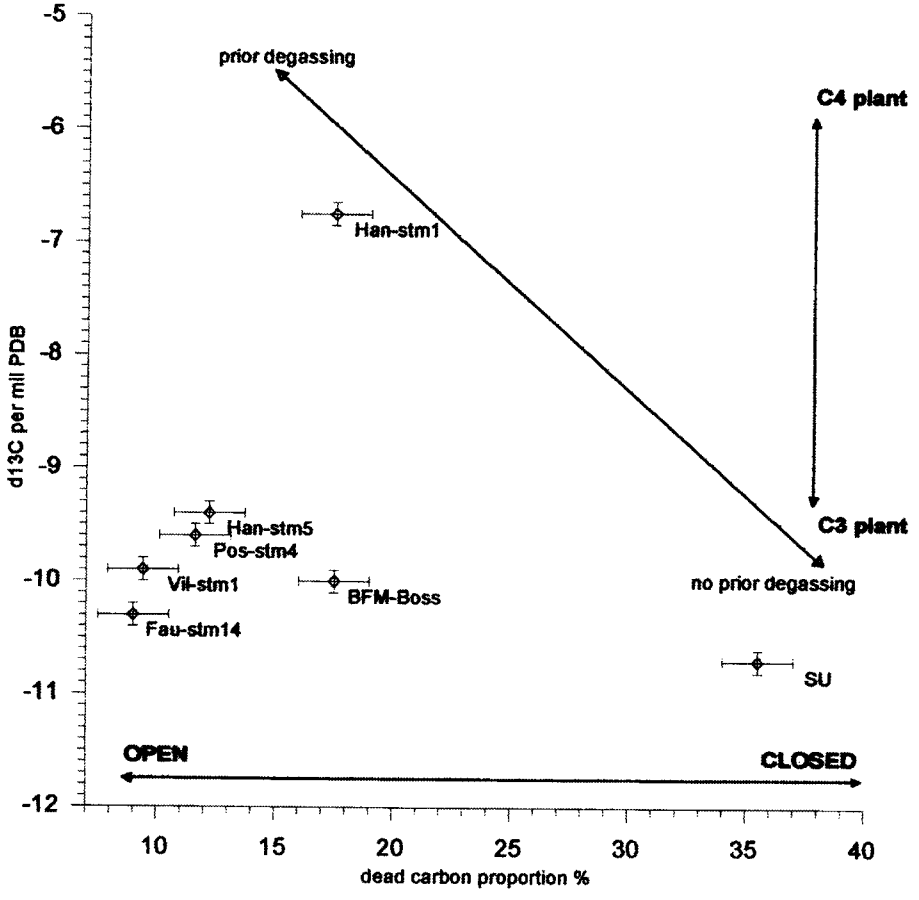

Figure 2 $\delta^{13}C$ vs. dcp; for Vil-stm1 and Han-stm1, dcp is the average of calculated past dcp (this study), for Fau-stm14, Pos-stm4, Han-stm5, BFM-Boss and SU the dcp has been calculated on modern stalagmites with the pre-bomb ^{14}C activity curve (see text, Table 8 and Genty et al. 1998; Genty and Massault 1999).

Several factors can explain the $\delta^{13}C$ and dcp values of the different samples: 1) change in the open/closed dissolution system proportion; 2) change in the type of vegetation (C3/C4) leading to a change in the soil CO_2 $\delta^{13}C$; or 3) possible degassing of the seepage water (and $CaCO_3$ precipitation) prior to entering the cave (Baker et al. 1997). The set of 5 stalagmites (Fau-stm14, BFM-Boss, Vil-stm1b, Pos-stm1 and Han-stm5) corresponds to caves that develop in limestone (Jurassic and Paleozoic). All are modern (i.e. <150 yr) except Vil-stm1b, whose mean dcp has been calculated on the last 3 ka. Soil that develops above these caves is thin (<30 cm thick), vegetation is varied and of

https://doi.org/10.1017/S003382220005712X Published online by Cambridge University Press

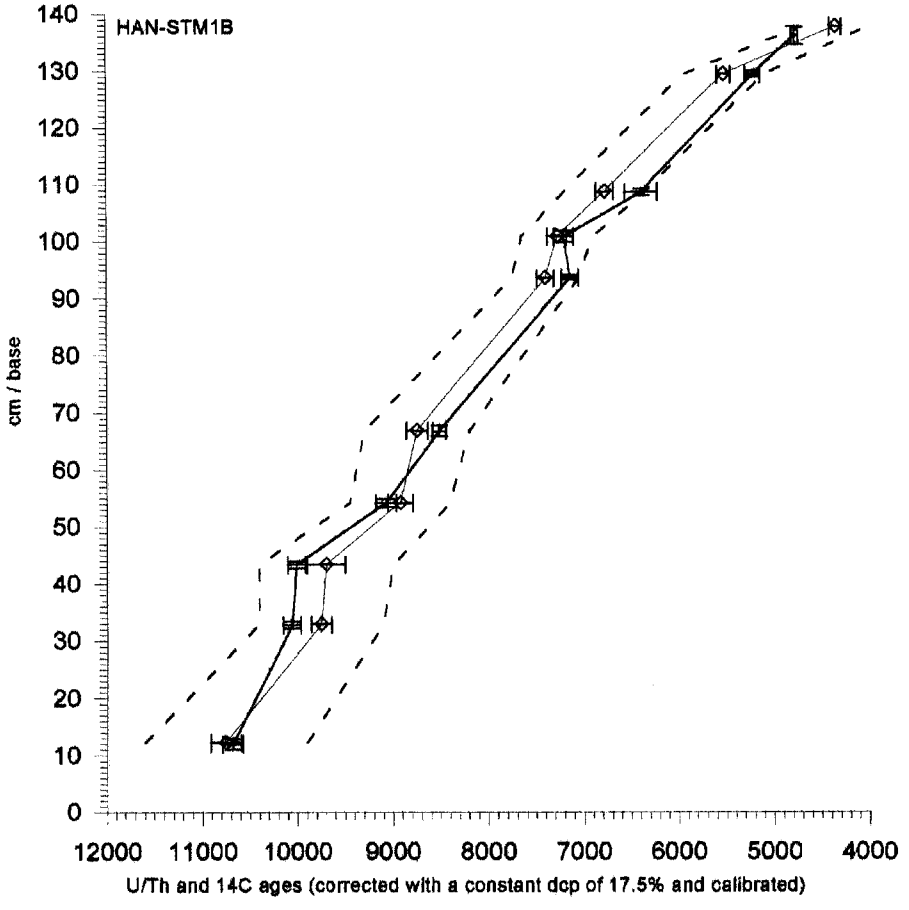

Figure 3 Growth curves of Han-stm1b stalagmite (Han-sur-Lesse Cave, Belgium). Note the very good correlation between ^{14}C (dcp corrected and calibrated ; diamonds and thin continuous line) and U/Th ages (thick continuous line). Dashed lines are error limits for ^{14}C ages, and have been calculated using an average dcp error of 1.5% and analytical errors (horizontal bars on diamonds).

the C3 type (deciduous woodlands and grasslands) and, despite slight variations in rainfall and temperature, climate is temperate and humid. Such environmental conditions seem to have favored an open-system dissolution process. The Han-stm1b sample comes from the same cave as one of the earlier samples (Han-sur-Lesse cave), but its average dcp and $\delta^{13}C$ were calculated on the first half of the Holocene. As explained earlier, the high $\delta^{13}C$ is difficult to interpret, but its dcp is in the range of the previous set. The SU-96-7 sample comes from a Scottish cave overlain by peat that develops in a dolomitic rock formation (Baker et al. 1993). The high SU-96-7 dcp value suggests that the dissolution system is almost closed. Its low $\delta^{13}C$ (–10.7‰ ±0.1) is likely the consequence of closed-system conditions and the very low soil CO_2 $\delta^{13}C$ (–29‰; Baker et al. 1999). These particular conditions are the consequence of a peat layer overlying the cave that is 60–100 cm thick and always saturated at the base; this prevents the occurrence of open-system conditions.

https://doi.org/10.1017/S003382220005712X Published online by Cambridge University Press

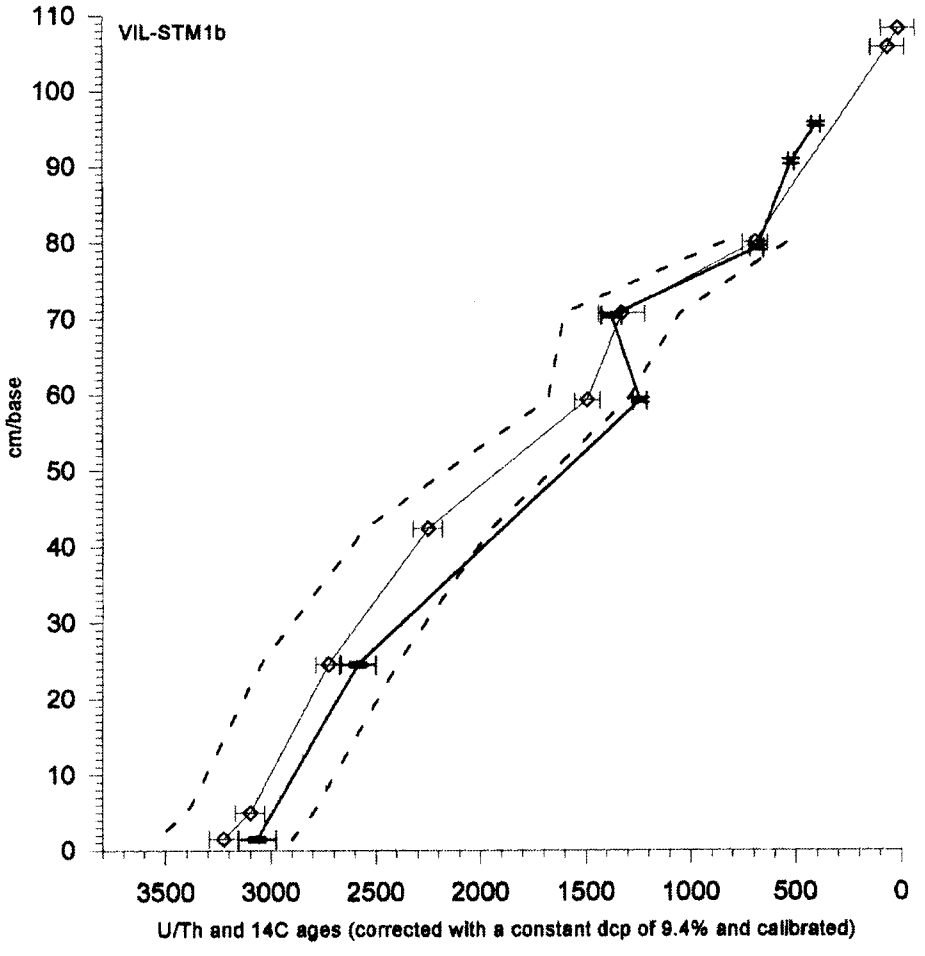

Figure 4 Growth curves of Vil-stm1b stalagmite (Villars Cave, SW France). Except 1 sample, the correlation between ^{14}C (dcp corrected and calibrated; diamonds and thin continuous line) and U/Th ages (thick continuous line) is very good. Dashed lines are error limits for ^{14}C ages, and have been calculated using an average dcp error of 1.5% and analytical errors (horizontal bars on diamonds).

Dead Carbon Proportion Time Variation

Despite the high dcp errors (Figure 1), one notes a broad parallel time variation of dcp and $\delta^{13}C$ on the Han-stm1b stalagmite. This is particularly visible between 10 ka and 7.2 ka, when dcp increases from 14.2% to 20.5% (6.3%), and $\delta^{13}C$ increases from –7.4‰ to –6.3‰ (0.9‰). These dcp and $\delta^{13}C$ variations might be the consequence of a vegetation change that occurred during this period in Belgium (Bastin 1990; Bastin and Gewelt 1986; Blanchon and Shaw 1995; Dansgaard et al. 1989; Lamb 1995), but because errors are large and because we have only one example, such a hypothesis needs confirmation.

The Vil-stm1b stalagmite shows a significant increase of $\delta^{13}C$ (3.3‰) between 760 AD and 1315 AD. This increase coincides with a slight dcp decrease that might not be significant, as it is within the error margin. We plan further measurements to try to interpret this $\delta^{13}C$ shift.

https://doi.org/10.1017/S003382220005712X Published online by Cambridge University Press

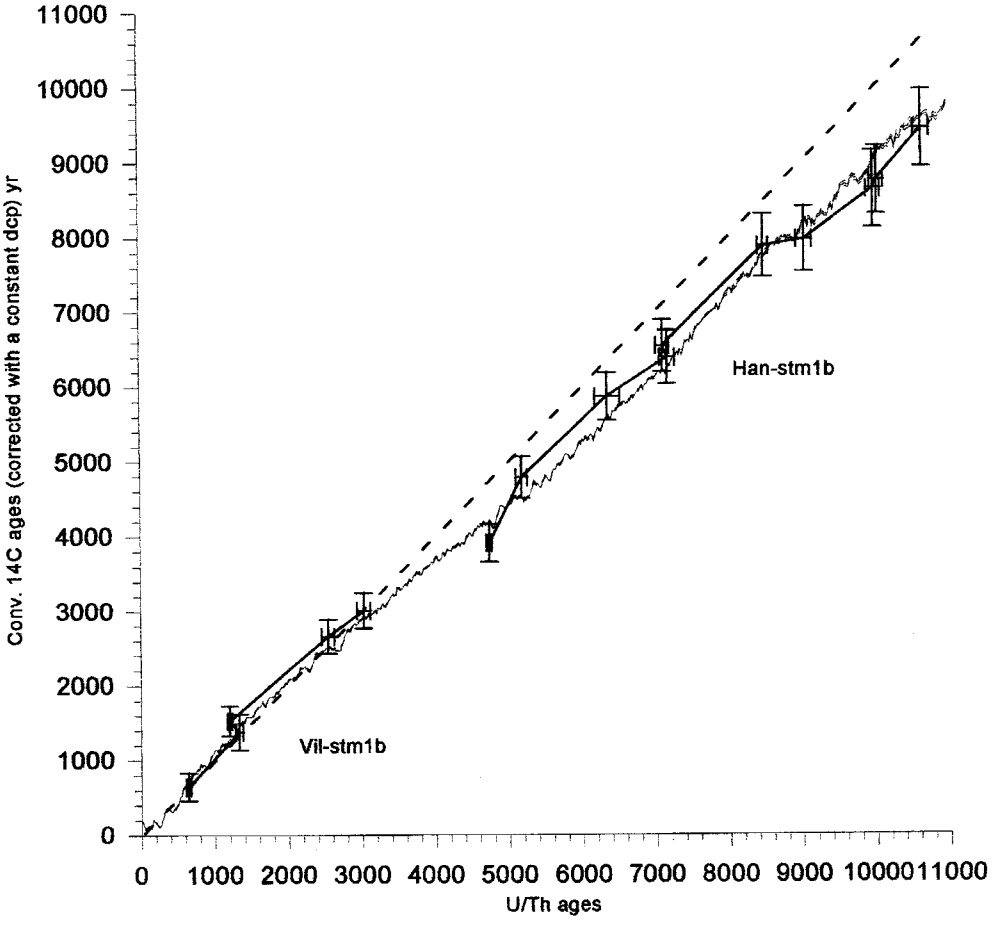

Figure 5 Comparison of conventional ^{14}C ages (dcp corrected), U/Th ages (of Han-stm1b and Vil-stm1b stalagmites), and calibration curve from dendrochronology (Stuiver and Kra 1986). Note the good fit between our measurements and the calibration curve.

Is ^{14}C AMS Suitable for Dating Speleothems?

Comparison between ^{14}C and U/Th ages on speleothems has not always produced similar results, even after dcp correction and calibration. In a Late Pleistocene stalagmite from Botswana (LII4, Lobatse II Cave), ^{14}C ages are younger than U/Th ages by 5–10 ka. This was explained by post-depositional introduction of younger ^{14}C and by increased atmospheric ^{14}C concentration (Holmgren et al. 1994). Conversely, a stalagmite from the Cracow-Wielun Upland area (Poland) showed a much older ^{14}C age (23 ka ± 0.2) than the U/Th age (18 ka ± 0.8); this discrepancy has not found a satisfactory explanation, but may be due to some unproven diagenetic processes (Pazdur et al. 1995).

We have compared here TIMS U/Th and AMS ^{14}C ages corrected by a constant dcp (average of the dcp_{past}: 17.5% for Han-stm1b, and 9.4% for Vil-stm1b). Results obtained show that except for the U/Th-F sample of the Vil-stm1b stalagmite, all TIMS U/Th ages are within the ^{14}C error margins (Figures 3 and 4). The correlation between the U/Th ages and the ^{14}C ages (dcp corrected and cali-

brated) is particularly good for the Han-stm1b stalagmite ($R^2 = 0.99$; n = 10; Figure 3). Consequently, it is tempting to say that ^{14}C AMS is a good method for dating stalagmites. However, the following problems still need to be considered:

1. To assume a constant dcp, this must be estimated by another means on a modern speleothem which can be a recent stalagmite or the top of an active one. Thus, the dcp can be calculated with the pre-bomb ^{14}C activity value;
2. If we consider a constant dcp, as above, the error on the ^{14}C age will be controlled by the error made on the modern dcp, which is about ±1.5% (Genty and Massault 1997). This leads to an age error between 250 and 500 yr for the Holocene (Tables 1 and 2). However, as we have demonstrated here, the dcp can vary by more than 6% (Figure 1), and then the real uncertainty is much higher and is dependent upon the unknown dcp_{past} variability.

Are Stalagmites Suitable for the Construction of Calibration Curves?

One of the first comparisons between these 2 dating methods (U/Th and ^{14}C) was made on a stalagmite from the Cango Cave (South Africa) and this suggested that between 30 and 40 ka BP, the level of ^{14}C in the atmosphere was higher (Vogel 1983). More recently on a stalagmite from the same site, a calibration curve (conventional ^{14}C ages vs. Uranium Series age) was established between 20 ka and 50 ka BP, which demonstrated the potential of speleothems for the reconstruction of past atmospheric ^{14}C activity (Vogel and Kronfeld 1997).

Our results show that AMS ^{14}C (dcp corrected with mean dcp_{past}) and TIMS U/Th ages fit relatively well with the calibration curve; data points are parallel to the curve within the error margin and we note that well pronounced variations of the calibration curve are followed by our data (for example the small "plateau" between 8200 and 9000 yr; Figure 5). However, for the Holocene, it appears that speleothems will not improve the accuracy of calibration curves, for at least 2 main reasons: analytical dcp error, and dcp variability.

For Holocene samples, analytical error is typically ±0.7 pMC for AMS ^{14}C, which is equivalent to an age error of ±60 yr. As explained above, the ^{14}C age error is between 250 and 500 yr (for the Holocene) if we suppose a constant dcp with an error of ±1.5%. But, we have shown here that despite the large errors made on dcp_{past} (averages are ±3.9% and ±2.8% for Vil-stm1b and Han-stm1b, respectively), it is likely that dcp has varied over time by several percent (6% in Han-stl1b stalagmite; Figure 1). Consequently, the total error must be much higher. Compared to errors made on existing calibration curves (between ±10 yr and ±60 yr for the Holocene), the error on speleothem samples is much too high for the improvement of the accuracy of such curves.

For the Glacial and Late Glacial periods, however, ^{14}C analytical errors increase (for example, between 50 yr and 490 yr in the V3 Cango stalagmite for ages <40 ka; Vogel and Kronfeld 1997) and consequently, relative dcp error decreases. For these times beyond the range of dendrochronological calibration, errors made on speleothems are comparable to errors made on other materials used for calibration curves (corals, lake sediment macrofossils; Bard et al. 1990; Kitagawa and Van der Plicht 1998). Thus, if the dcp did not change more than ±3% as observed in Han-stm1b, speleothems would be good tools for the construction of calibration curves. However, we must keep in mind that 2 important problems remain: 1) finding speleothems that grew during glacial periods, which probably means low latitude areas (Lauritzen et al. 1990, 1995); and 2) ensuring that dcp did not change significantly (i.e. more than the amount observed in Han-stm1b stalagmite), which might not be likely during climatic transitions as we know that between glacial and Holocene periods, vegetation and climatic conditions changed significantly.

CONCLUSION

This study demonstrates that:

1. Calibrated AMS ^{14}C ages, which have been corrected assuming a constant dead carbon proportion, show good agreement with TIMS U/Th ages. However, when taking into account the error estimated on the dcp, this will increase the final error on the ^{14}C age by about a factor of 3;
2. In the 2 stalagmites studied, the dead carbon proportion did not change significantly during the Holocene; we estimate 9.4% (σ=1.6; n= 6) for Vil-stm1b stalagmite and 17.5% (σ=2.4; n=10) for Han-stm1b stalagmite. The difference between the 2 stalagmites is due to differences in the limestone dissolution process, which is controlled by vegetation dynamics, climatic conditions and geological settings as demonstrated by the $\delta^{13}C$ data. Comparison with other stalagmites where dcp and $\delta^{13}C$ have been calculated demonstrate the variability and the complexity of the dissolution processes from open to closed system conditions.
3. In the Han-stm1b stalagmite, despite the broad stability observed (17.5% ±2.4%), dcp has increased by more than 6% between 10 ka and 7.2 ka and remained high until 5.2 ka. This increase is accompanied by an increase in the calcite $\delta^{13}C$ of 0.9‰. This could be the consequence of a more intense dissolution process likely due to a change in the vegetation cover; but more information is needed to confirm this hypothesis.
4. Calibrated AMS ^{14}C ages, corrected with a constant dcp, show an excellent correlation with the TIMS U/Th ages (R^2=0.99); consequently, provided that the dcp can be calculated on a modern part of a stalagmite (with the pre-bomb calcite ^{14}C activity value) and that the past dcp remains in the ±3% range variability observed in our samples, the ^{14}C AMS technique can be a good tool for the dating of the stalagmites, and despite the fact that dcp error greatly increases the error made on the age, this technique still has the advantages of simplicity, requiring very little matter, and a low price;
5. Using speleothems as a tool for establishing calibration curves is confronted by 2 problems: 1) the ^{14}C age error, which is much higher, at least for the Holocene, than the error found in the already published curves; and 2) the hypothesis of a constant dcp, which is needed to reconstruct past atmospheric ^{14}C activity, and which is unlikely, especially during climatic transitions.

ACKNOWLEDGMENTS

This study was funded by specific research programs of the Centre National de la Recherche Scientifique: DBT, DYTEC, VariEnte and GDR 970. It is part of IGCP 379 and PAGES PEPIII programs. We are grateful to those who helped us in sampling: Thierry Baritaud, Yves Quinif, Guy Deflandre and to cave owner Hubert Versaveau, and for the helpful comments of Claude Hillaire-Marcel and Bassam Ghaleb.

REFERENCES

Baker A, Smart PL, Edwards RL, Richards DA. 1993. Annual growth bandings in a cave stalagmite. *Nature* 364:518–20.

Baker A, Genty D, Dreybrodt W, Barnes W, Mockler N, Grapes J. 1997. Testing theoretically predicted stalagmite growth rate with Recent annually laminated samples: implications for past stalagmite deposition. *Geochimica et Cosmochimica Acta* 62: 393–404.

Baker A, Genty D. 1999. Fluorescence wavelength and intensity variations of cave waters. *Journal of Hydrology* 217:19–34.

Baker A, Ito E, Smart PL, McEvan R. 1997. Elevated ^{13}C in speleothem and implications for palaeovegetation studies. *Chemical Geology* (Isotope Geoscience) 136: 263–70.

Baker A, Caseldine CJ, Gilmour MA, Charman D, Proctor CJ, Hawkesworth CJ, Phillips N. 1999. Stalagmite luminescence and peat humification records of palaeomoisture for the last 2,500 years. *Earth and Planetary Science Letters* 165:157–62.

Bard E, Hamelin B, Fairbanks RG, Zindler A. 1990. Calibration of the ^{14}C timescale over the past 30,000 years

using mass spectrometric U-Th ages from Barbados corals. *Nature* 345:405–10.

Bar-Mattews M, Ayalon A, Mattews A, Sass E, Halicz L. 1996. Carbon and oxygen isotope study of the active water-carbonate system in a karstic Mediterranean cave: implications for paleoclimate research in semi-arid regions. *Geochimica et Cosmochimica Acta* 60: 337–47.

Baskaran M, Krishnamurphy RV. 1993. Speleothems as proxy for the carbon isotope composition of atmospheric CO_2. *Geophysical Research Letters* 20: 2905–8.

Bastin B. 1990. L'analyse pollinique des concrétions stalagmitiques: méthodologie et résultats en provenance des grottes belges. *Karstologia Mémoires* 2: 3–10.

Bastin B, Gewelt M. 1986. Analyse pollinique et datation ^{14}C de concrétions stalagmitiques holocènes: apports complémentaires des deux méthodes. *Géographie Physique et Quaternaires* 15(2):185–96.

Blanchon P, Shaw J. 1995. Reef drowning during the last deglaciation: evidence for catastrophic sea-level rise and ice-sheet collapse. *Geology* 23:4–8.

Broecker WS, Olson EA. 1960. Radiocarbon measurements and annual rings in cave formations. *Nature* 185: 93–4.

Bronk RC. 1994. analysis of chronological information and radiocarbon calibration: the program OxCal. *Archaeological Computing Newsletter* 41:11–6.

Dansgaard W, White JWC, Johnson SJ. 1989. The abrupt termination of the Younger Dryas climatic event. *Nature* 339:532–3.

Dever L, Durand R, Fontes J-C, Vachier P. 1982. Géochimie et teneurs isotopiques des systèmes saisonniers de dissolution de la calcite dans un sol sur craie. *Geochimica et Cosmochimica Acta* 46: 1947–56.

Dörr H, Münnich KO. 1986. Annual variations of the ^{14}C content of soil CO_2. *Radiocarbon* 28(2A): 338–45.

Drake JJ. 1983. The effect of geomorphology and seasonality on the chemistry of carbonate groundwater. *Journal of Hydrology* 61:223–36.

Drake JJ. 1984. Theory and model for global carbonate solution by groundwater. In: RG LaFleur, editor. *Groundwater as a geomorphic agent.* London, Allen & Unwin. p 210–26.

Dulinski M, Rozanski K. 1990. Formation of $^{13}C/^{12}C$ isotope ratios in speleothems: a semi-dynamic model. *Radiocarbon* 32(1):7–16.

Edwards RL, Chen JH, Wasserberg GJ. 1987. ^{238}U-^{234}U-^{232}Th-^{230}Th, systematics and precise measurement of time over the last 500,000 years. *Earth and Planetary Science Letters* 81:175–192.

Fleyfel M. 1979. Etude hydrologique, géochimique et isotopique des modalités de minéralisation et de transfert du carbone dans la zone d'infiltration d'un aquifère karstique: le Baget (Pyrénées ariégeoises) [dissertation]. Paris, Université P. et M. Curie. 221 p.

Fleyfel M, Bakalowicz M. 1980. Etude géochimique et isotopique du carbone mineral dans un aquifere karstique. 1980 Nov 17–18. Bordeaux: Colloque Société Géologique de France. 231–45.

Fritz P, Reardon EJ, Barker EJ, Brown M, Cherry A, Killey WD, McNaughton D. 1978. The carbon isotope geochemistry of a small groundwater system in northeastern Ontario. *Water Resources Research* 14:1059–67.

Gascoyne M, Nelson DE. 1983. Growth mechanisms of recent speleothems from Castelguard Cave, Columbia Icefields, Alberta Canada, inferred from a comparison of Uranium-series and Carbon-14 data. *Artic and Alpine Research* 15:537–42.

Gascoyne M. 1992. Paleoclimate determination from cave calcite deposits. *Quaternary Science Reviews* 11: 609–32.

Genty D, Quinif Y. 1996. Annually laminated sequences in the internal structure of some Belgian stalagmites – Importance for paleoclimatology. *Journal of Sedimentary Research* 66:275–88.

Genty D. Baker A. Barnes W, Massault M. 1996. Growth rate, grey level and luminescence of stalagmite laminae: Climate Change: The Karst Record. Proceedings of the symposium in Bergen. 1996 Aug 1–4; Norway. University of Bergen, Norway. *Karst Water Institute Special Publication* 2. 36–9.

Genty D, Massault M. 1997. Bomb ^{14}C recorded in laminated speleothems: dead carbon proportion calculation. *Radiocarbon* 39(1):33–48.

Genty D, Baker A, Barnes W. 1997. Comparaison entre les lamines luminescentes et les lamines visibles annuelles de stalagmites. *Comptes Rendus de l'Académie des Sciences de Paris* 325:193–200.

Genty D, Vokal B, Obelic B, Massault M. 1998. Bomb ^{14}C time history recorded in two modern stalagmites – Importance for soil organic matter dynamics and bomb ^{14}C distribution over continents. *Earth and Planetary Science Letters* 160:795–809.

Genty D, Massault M. 1999. Carbon transfer dynamics from bomb-^{14}C and $\delta^{13}C$ time series of a laminated stalagmite from SW-France – Modelling and comparison with other stalagmite. *Geochemica et Cosmochemica Acta.* Forthcoming.

Gewelt M. 1986. Datation ^{14}C des concrétions de grottes belges: vitesses de croissance durant l'Holocène et implications paléoclimatiques. In: Patterson K, Sweeting MM, editors. *Proceedings of the Anglo-French Karst Symposium (1983).* Norwich: Geo. Books. p 293–322.

Geyh MA, Henning GJ. 1986. Multiple dating of a long flowstone profile. Radiocarbon 28(2A):503–9.

Hendy CH. 1971. The isotopic geochemistry of speleothems-I. The calculation of the effects of different modes of formation on the isotopic composition of speleothems and their applicability as paleoclimatic indicators. *Geochimica et Cosmochimica Acta* 35: 801–24.

Holmgren K, Lauritzen SE, Possnert G. 1994. $^{230}Th/^{234}U$ and ^{14}C dating of a Late Pleistocene stalagmite in Lobatse II cave – Botswana. *Quaternary Geochronology* 13:111–9.

Kitagawa H, Van der Plicht J. 1998. Atmospheric radiocarbon calibration to 45000 yr BP. late gacial fluctuations and cosmogenic isotope production. *Science* 279:1187–90.

Lamb HH. 1995. *Climate history and the modern world.* London and New York, Routledge. 432 p.

Lauritzen SE, Lovlie R, Moe D, Ostbye E. 1990. Paleoclimate deduced from a multidisciplinary study of a half-million-year-old stalagmite from Rana, Northern Norway. *Quaternary Research* 34: 306–6.

Lauritzen SE. 1995. High-resolution paleotemperature proxy record for the last interglaciation based on Norwegian speleothems. *Quaternary Research* 43:133–46.

Liu T, Tan M, Qin X, Zhai S, Li T, Lü J, De'er Z. 1997. Discovery of microbedding in speleothems in China and its significance in the study of Global Change. *Quaternary Science* (China) 2:41–51.

Mangin A. 1975. Contribution à l'étude des aquifères karstiques [dissertation]. Université de Dijon.

Mook WG, Bommerson JC, Staverman WH. 1974. Carbon isotope fractionation between dissolved bicarbonate and gaseous carbon dioxide. *Earth and Planetary Science Letters* 22:169–76.

Mook WG. 1980. Carbon 14 in hydrogeological studies. In: Fritz P, Fontes J-Ch, editors. *Handbook of Environmental Geochemistry* 1A:49–74.

Pazdur A, Pazdur MF, Pawlyta J. 1995. Paleoclimatic implications of radiocarbon dating of speleothems from the Cracow-Wielun upland, southern Poland. *Radiocarbon* 37(2):103–10.

Railsback LB, Brook GA, Chen J, Kalin R, Fleisher CJ. 1994. Environmental controls on the petrology of a late Holocene speleothem from Botswana woth annual layers of aragonite and calcite. *Journal of Sedimentary Research* A64(1):147–55.

Shopov YY, Dermendjiev V. 1990. Microzonality of luminescence of cave flowstones as a new indirect index of solar activity. *Compte Rendu de l'Académie Bulgare des Sciences* 43:9–12.

Stuiver M, Kra RS, editors. 1986. Calibration issue. *Radiocarbon* 28(2B):805–1030.

Talma AS, Vogel JC. 1992. Late Quaternary paleotemperatures derived from a speleothem from Cango Caves, Cape Province, South Africa. *Quaternary Reasearch* 37:203–13.

Tan M. Liu T. Quin X, De'er Z. 1997. Microbanding of stalagmite and its significance. *PAGES Report* 5:6–7.

Vogel JC. 1983. ^{14}C variations during the Upper Pleistocene. *Radiocarbon* 25(2):213–8.

Vogel JC, Kronfeld J. 1997 Calibration of radiocarbon dates for the Late Pleistocene using U/Th dates on stalagmites. *Radiocarbon* 39(1):27–32.